Absolute Quantification of Gene Expression in Individual Bacterial Cells Using Two Photon Fluctuation Microscopy

Matthew L. Ferguson[a], Dominique Le Coq[b], Matthieu Jules[b], Stéphane Aymerich[b], Nathalie Declerck[a,b] & Catherine A. Royer[a]

[a]Centre de Biochimie Structurale, INSERM U554, CNRS UMR 5048, Université Montpellier 1 and 2, F-34090 Montpellier, France

[b]INRA UMR1319 Micalis, Domaine de Vilvert, F-78350 Jouy-en-Josas, France.

ABSTRACT Quantification of promoter activity or protein expression in gene regulatory networks is generally achieved via measurement of fluorescent protein (FP) intensity by flow cytometry or wide field or confocal microscopy. The FP intensity measured in single cells is related to the true FP concentration by an unknown scaling factor, hence limiting the level of analysis and interpretation. Here, using approaches originally developed for eukaryotic cells, we show that two-photon (2p) fluorescence fluctuation microscopy, and specifically scanning Number and Brightness (2psN&B) analysis, can be applied to determine the absolute concentrations of diffusing FPs in live bacterial cells. First, we showed that the open fluctuation volume must be significantly smaller than the width of the bacterium, attained here with a 2-photon microscope perfectly aligned to the diffraction limit. We demonstrate by Brownian dynamics simulations that our 0.07 fL 2p-excitation volume (vol_{ex}) is sufficiently small so as to provide 93% accuracy in the brightness value. The lack of spatial heterogeneity of the FP molecular brightness observed within or among individual bacterial cells bearing FP promoter fusions allowed us to perform spatial averaging, without which absolute numbers measurements cannot be made. Next, we showed that correct calculations of the true FP concentration in each cell require use of only the central pixels of the bacteria, for which the excitation volume is encompassed in the cell. We established the lower detection limits for GFP molecules diffusing in bacteria, which thanks to the very low auto-fluorescence with infra-red excitation, is at or below 75 nM (~3 molecules of FPs /vol_{ex}). Above the upper limit of fluctuation approaches (~10 μM), reliable estimates of FP concentrations can be retrieved from fluorescence intensities using the molecular brightness values determined at low concentrations. We found that the uncertainty inherent to our measurements (< 5%) was much smaller than the very high cell-cell variations observed for stochastic leakage from FP fusions of the *lac* promoter in the repressed state, or even the 10-25% variation observed upon induction. This demonstrates that reliable and absolute measure of transcriptional noise can be made using our approach, which should make it particularly appropriate for the investigation of stochasticity in gene expression networks.

Introduction

Quantification of gene expression at the single cell level is key to understanding, predicting and eventually modulating growth, development, and adaptation of cell populations and organisms (1, 2). Cell-to-cell variations in the abundance of gene products reflect the stochastic noise inherent to the biochemical processes of gene expression and regulation networks, as well as random fluctuations in cellular components and physiological or environmental factors. Investigations of this type typically use flow cytometry or wide field or confocal microscopy to measure the intensity of emission of fluorescent proteins (FPs) expressed from promoter or gene fusions, or of single mRNA molecules by in situ hybridization with fluorescent oligonucleotides (for example see (3-5)). In these approaches, the measured fluorescence signal is considered to be proportional to the intracellular concentration of fluorescent molecules, but does not yield their concentration directly. The scaling factor that relates the fluorescence intensities to the actual protein copy number is usually not known or estimated indirectly using *in vitro* or *in vivo* calibration methods, hence limiting the extent to which the data can be interpreted. In addition, differences in intrinsic brightness are not considered. And, the detection limits of these techniques are often restricted by the relatively high auto-fluorescence of the bacterial cytoplasm, or because of photo-bleaching or long-range contaminating fluorescence emanating from bright cells. In the case of immobile molecules (6, 7), or alternatively, calibration from immobile particles (8), particle counting and noise measurements are possible down to one molecule per cell. However, the requirement for immobility is not always desirable, as it relies on either highly localized protein fusions or fixed cells.

In the present work we test the capacity of fluorescence fluctuation methods to provide an absolute and quantitative measure of gene expression in live bacterial cells. We have imaged and analyzed individual cells of the model Gram positive bacterium *Bacillus subtilis* producing fluorescent reporter proteins under the control of inducible promoters. We first demonstrate that fluorescence correlation spectroscopy (FCS) (9, 10) acquired at single points is not ideally suited to our present application due to photobleaching of the FP molecules associated with their confinement inside the small bacterial cells. Successful implementation of fluctuation analysis in this context required the use of two-photon excitation coupled to an image scanning fluctuation approach termed scanning Number and Brightness (11, 12). This method should not be confused with approaches that quantify the fluctuations in total cell fluorescence intensity upon cell division as a mean to determine the conversion factor of fluorescence signal to protein copy number (13, 14). In two-photon scanning number and brightness (2psN&B), we measure the fluorescence fluctuations that arise from Brownian diffusion into and out of the very small excitation volume focused inside the bacterial cell. Two-photon excitation minimized the fluctuation volume, as well as the auto-fluorescence from the bacterial cells, while scanning N&B eliminated the photobleaching due to confinement that precluded point-based methods. We describe a number of essential modifications to N&B, a technique originally developed in eukaryotic systems, which were necessary for its implementation with bacterial transcriptional FP fusions. First we showed that these absolute measurements required careful consideration of the specific geometric relationships between the bacteria and the two-photon excitation volume, as well as perfect diffraction limited alignment of a two-photon microscope. Second,

we showed that the spatial averaging of the shot-noise corrected pixel-based molecular brightness values is required for reliable calculation of absolute protein concentrations. Third, we demonstrated that accurate determinations of absolute FP concentration could only be achieved using the central 50% of bacterial pixels. Next, we established the upper and lower limits to the approach, and the degree of uncertainty inherent to such measurements in bacteria. This combination allowed for the absolute quantification of the concentration of diffusing FP molecules in individual *B. subtilis* cells at very low levels and over a broad dynamic range. Measurements on large numbers of cells yielded highly accurate values of mean expression levels and the associated heterogeneity in the cell population. With the presently described modifications in data acquisition and analysis, our approach should prove to be broadly applicable as it involves simple scanning two-photon microscopy and GFP promoter fusion strains widely used in studies of gene regulatory networks.

Materials and Methods

Bacterial strains The *B. subtilis* strain GM2812 producing the green fluorescent protein (GFP) was obtained by transforming for spectinomycin resistance strain BSB168, a *trp+* derivative of the reference strain 168 Marburg (15), with plasmid pDR146 (a kind gift from D. Rudner, Harvard Medical School). This results in the integration by a double crossing-over into the chromosomal *amyE* locus of the *gfpmut2* gene placed under the control of the $P_{hyperspank}$ promoter, an IPTG-inducible promoter derived from the *E. coli lac* operon. Similarly, transformation of BSB168 for spectinomycin resistance with plasmid pIC626 gave the CFP-carrying strain GM2919, in which a $P_{hyperspank}$*cfp* transcriptional fusion is integrated in *amyE*, together with *lacI*, the *lac* repressor encoding gene from *E. coli*. Plasmid pIC626 was obtained by placing the *cfp* gene (codon-optimized for *B. subtilis*) under the control of the IPTG-regulated $P_{hyperspank}$ promoter through cloning of a *Hin*dIII-*Sal*I restriction fragment of pDR200 into pDR111 (both kind gifts from D. Rudner). As previously described, the transcriptional fusion of the *gapB* promoter with *gfpmut3* was constructed within the pBaSysBioII using ligation-independent cloning prior integration into the chromosome in a non-mutagenic manner and resulting in strain BBA9006 (16).

Cell cultures and sample preparation Protocols for media preparation and cell culture were adapted from previously described protocols (16) and the BaSysBio standardized procedures (http://www.basysbio.eu). For strains expressing the $P_{hyperspank}$ transcriptional fusions, cells from glycerol stocks were grown at 37°C for 2-3 hours in 2 mL LB medium supplemented with spectinomycin at 100 µg/ml and use to inoculate serial dilutions in minimal M9 medium containing 0.5% malate as a carbon source. After overnight growth at 30°C, one of the cultures in exponential phase (having an optical density at 600 nm (OD_{600}) between 0.2 and 0.6) was used to inoculate 5 mL of the same M9 medium supplemented with 0, 10, 100 or 1000 µM of IPTG. Cells were diluted to OD_{600} between 0.1 and 0.2 and grown in culture plate with shacking at 37°C. After 2 h induction, aliquots were removed from the cell cultures for preparing microscopy samples (see below), as well as for OD and bulk fluorescence measurement in 96 wells-microtiter culture plates using Saphir2 microplate reader (TECAN) and an excitation/emission wavelength of 485/528 nm for measuring GFP or 433/480 nm for measuring

CFP. For the strain expressing the P_{gapB}gfpmut3 transcriptional fusion at steady-state under glucose repression and balanced growth conditions, an overnight pre-culture was performed as above in M9 medium supplemented with spectinomycin and 0.5% glucose. One of the exponentially growing cultures was freshly diluted in the same medium and aliquots were removed after 2-3 h growth at 37°C.

For preparing samples for single cell analysis, 1 mL aliquots of the cell cultures were centrifuged at 13 000 rpm for 1 min, re-suspended in cold M9-medium to an OD of 20 and left on ice until microscopy measurements. Agarose pads were prepared by depositing 60 μL of 1.5% agarose -M9 medium (containing either 0.5% glucose or malate) on a glass coverslip to which a ring of 1x20mm double adhesive silicone spacer (Invitrogen, Carlsbad, CA) was attached. The agarose pad was allowed to dry in a laminar flow hood for 12 min after which the agarose was stiff enough to immobilize the bacteria and still large enough to touch a second coverslip applied on top. After sample preparation, 2-3 μL of the concentrated bacteria were quickly placed in the center of an agarose pad. Bacterial cells were allowed to sediment for 1 min after which the second glass coverslip was sealed. The sample was then placed in an AttoFluor cell chamber (Molecular Probes, Carlsbad, CA) and imaged quickly (within 15 min) under the microscope. This protocol allowed for a consistent monolayer of cells with an intermediate cell density.

Two-photon scanning microscopy Cells were imaged on an Axiovert 200M inverted microscope (Zeiss, Germany) equipped with an ISS laser scanning module and an ISS Alba (ISS, Champaign IL) with two channel APD detection. FPs were excited at 930nm with a femtosecond pulsed infrared Titanium Sapphire laser (Spectra Physics MaiTai, Newport, Mountainview CA). In the laser scanning module, 930 nm excitation light was expanded to fill the back aperture of a Zeiss Apochromat 63X, 1.4 NA, oil immersion objective. Laser power before injection into the laser scanning module was 15mW. This level of excitation intensity was chosen to provide the maximum count rate without photo-bleaching for *in vivo* GFP with a laser dwell time of 50μs. Infrared excitation light was filtered from the detection path by an E700 SP 2P dichroic filter. In order to eradicate excitation light from detection, a secondary E700 SP 2P filter was placed between the laser scanning module and the Alba. Photons were detected with a SPCM-AQR-15 APD (Perkin Elmer, Waltham, MA) with a dark count of 50 cps.

FCS Measurements The fluctuations in the fluorescence emission in a small open volume are detected and time-correlated generating the autocorrelation function $G(\tau)$:

$$G(\tau) = \frac{<\delta F(t)\delta F(t+\tau)>}{<F(t)>^2} \qquad (1)$$

where τ is the lag time. In the particular case of a system of freely diffusing species and assuming a 3D Gaussian excitation profile, closed form expressions are derived:

$$G(\tau) = G(0)\left(1+ \tau/\tau_D\right)^{-1}\left(1+ \varpi_0^2\tau/z_0^2\tau_D\right)^{-1/2} \quad (2)$$

where ω_o and z_o are the waist and length, respectively, of the three-dimensional Gaussian excitation volume at which the intensity drops to $1/e^2$. Here, τ_D is the translational diffusion time and *G(0)*, the amplitude of the auto-correlation functions which can be expressed as:

$$G(0) = \frac{1}{V_{eff}C} \quad (3),$$

where $V_{eff}=(\pi/2)^{3/2}\omega_0^2 z_0$ and *C* is the concentration of the fluorescent species.

Number and Brightness In scanning Number and Brightness (N&B) analysis (11, 12) the shot noise corrected true number, n, and brightness, ε, of the diffusing fluorescent molecules are calculated from the fluctuations in fluorescence intensity at each pixel in a series of raster scanned images, in which the pixel dwell time is small with respect to the diffusion time of the molecule.

$$\varepsilon = [(F_{(i)}-\langle F\rangle)^2 - \langle F\rangle]/\langle F\rangle \quad (4)$$

$$n = \langle F\rangle^2/[(F_{(i)}-\langle F\rangle)^2 - \langle F\rangle] \quad (5).$$

The subscript, *i*, refers to the raster scanned image number from 1 to 50. For each field of view, we imaged 50 frames of a 20μm x 20μm area. Photon counts were registered in a 256x256 pixel image while raster scanning the laser with a 50μs laser dwell time per pixel. The laser dwell time (50 μs) was chosen with to be faster than the FP diffusion and to provide statistically relevant photon counts while reducing the effects of photo-bleaching. Analysis was carried out using programs written in IDL 6.0 (ITT Visual Information Solutions, Boulder, CO).

Brownian Dynamics Simulations A three dimensional particle trajectory was generated by the addition of a uniformly distributed random number with a mean value of zero and variance of $\sqrt{2D}$ dt to each coordinate at each time step (17). The coefficient of diffusion, D, was fixed at 10 $\mu m^2/s$ and the time step, dt, was fixed at 50 μs for N&B. If the particle reached the cell wall, the component of the displacement vector normal to the cell wall for that time step was reflected. It was estimated that a 10 second trajectory would be sufficient sampling for a single particle trajectory with reflective boundary conditions in a 1 fL bacterial cell (a=0.34μm and b=1.5μm). The simulated fluorescence intensity, F(x,y,z,t), was calculated from the trajectory by assigning a value of 1 or 0 depending on whether a randomly drawn number was less than or greater than the two photon excitation probability, $P(x,y,z,w_0,z_0)=\exp(-4x^2/w_0^2-4y^2/w_0^2-4z^2/z_0^2)$, defined by the position of the particle with respect to the center of the excitation volume. By centering the excitation volume at different locations within the bacterial cell we were able to

compute the theoretical cell profile by Number and Brightness analysis. This calculation was then used to estimate the error in averaging over different fractions of pixels within the cell (Data not shown). We found that the best compromise between statistical error and smoothing was to use the inner 50% of the cell when determining intracellular concentration. By varying the size of the excitation volume both in the focal plane and azimuthal direction, we were able to estimate the effect of confinement on Number and Brightness measurements.

Results and Discussion

Imaging FP-producing bacteria by two photon microscopy. Two-photon (2p) microscopy has been widely used for imaging eukaryotic cells because it provides 3D resolution that is comparable to confocal microscopy, while producing less photo-damage and allowing better tissue penetration (for review see e.g.(18, 19))). In contrast, 2p microscopy has not yet been used for quantitative studies of bacterial systems at the level of single cells, although we found it presents several advantages compared to the one-photon mode. Here we have imaged agarose immobilized live cells of the *B. subtilis* 168 (BSB168) strain carrying a chromosomal *gfpmut2* (encoding a highly stable and bright GFP variant (20)) or a codon-optimized *cfp* (encoding a cyan GFP variant) under the control of the IPTG-inducible $P_{hyperspank}$ promoter. Comparison of the average fluorescence intensities recorded in 50 scan frames of cells expressing GFP as a function of IPTG concentration is shown in Figure 1A (note the difference in full scale between panels). We observed significant heterogeneity in fluorescence for the un-induced cells (first panel in Figure 1A), reflecting important cell-cell variations in transcription leakage from the repressed promoter. Addition of increasing concentrations of IPTG to the culture medium resulted in increasingly bright and more homogeneous bacterial cells after only two hours of induction. The average fluorescence measured in the individual cells was compared to that observed in bulk measurements of the same bacterial samples using a fluorescence microplate reader (Figure 1B). The relative fluorescence intensities determined by the two methods are well correlated except for low values where the rather high auto-fluorescence of the receiver BSB168 strain observed in bulk measurements precludes accurate quantification of FPs basal expression. In contrast, a near zero level of background fluorescence is observed for the BSB168 strain in the two photon scanning measurements, allowing detection of promoter activity under un-induced conditions. Moreover a much larger standard deviation is observed in the single cell measurements, reflecting the stochastic noise inherent to the biological system. Finally, in the individual cell measurements, we found that the average fluorescence for the CFP producing strains is five-fold lower than that observed for GFP, although from intensity values it is not possible to ascertain whether this is due to differences in protein expression levels between the two FPs, or alternatively to a difference in their individual molecular brightness.

Another advantage of two-photon over the wide field or confocal microscopy methods typically used in such studies lies in the lack of “halo” effect in the evaluation of the fluorescence emitted by single cells. When mixtures of cells from the BSB168 receiver strain (containing no FP encoding gene) and the fully induced GFPmut2 producing strain are imaged

(Figure 1C, note the 100-fold difference in scales in the left panel for the two cell-types), the boundaries between bright cells are well defined (Figure 1C, right top panel), and the very low intensity in the center of the very dim cells is not contaminated by intensity from neighboring bright cells (Figure 1C, right bottom panel). Although resolution in two photon excitation is lower in principle than for confocal or wide field microscopy because of the longer excitation wavelength, in practice, the fact that infinitely small pinholes are not used generally in confocal systems, the lack of Stokes shift effect in 2p, the quadratic dependence of the emission on 2p excitation power and the low background and scattering thanks to the longer wavelengths provides generally somewhat better resolution in two-photon mode (21). Based on fluorescence intensity profiles as shown in Fig. 1C, we determined the average size of the bacterial cytoplasm of *B. subtilis*. The length of individual cells of this rod-shape bacterium greatly varied (from 0.5 to over 4 μm) depending on the cell cycle and growth conditions, whereas the cell internal diameter remained fairly constant, averaging at 0.7 μm.

Fluctuation methods, the excitation volume and bacterial geometry More powerful than simple intensity measurements, fluorescence fluctuation microscopy allows for the counting of the actual number of molecules in the excitation volume, and hence determination of their absolute concentration and molecular brightness. Such absolute quantification of promoter activity is highly desirable in the context of gene expression networks. Fluctuation based particle counting relies on the fact that the number of particles diffusing through a small open volume in an infinitely large reservoir obeys Poisson statistics (for a recent review see (10)). However, given the size of the two-photon excitation function with respect to the bacterial cells, this assumption may not be entirely valid in the present case, and confinement results in reflective boundary conditions. Hence, we sought to determine the extent to which the small size of the bacterial cytoplasm (in the range of 1 fL) would affect the fluctuation measurements.

The effective two-photon excitation volume V_{eff} can be approximated by a 3D Gaussian function which is defined by the parameters ω_0 and z_0. These parameters define the full width at half maximum of the emission photon density (or alternatively the distance at which the photon density decays by $1/e^2$) in the focal plane and the azimuthal direction, respectively. We distinguish the excitation profile from the diffraction limited PSF because of the quadratic dependence of excitation probability on intensity in two-photon excitation. The ω_0 and z_0 values of our two-photon V_{eff} exciting at 930 nm were determined using the G(0) value of the autocorrelation function obtained by fluorescence correlation spectroscopy (FCS) measurements. In order to mimic the conditions inside the bacterial cytoplasm, two solutions of rhodamine 110 at 16 nM and 160 nM were measured in 75% glycerol to increase the diffusion time to ~1 ms. The value of ω_o was found to be 0.34 μm and the z_0 value, 1.4 μm (V_{eff} = 0.31 fL). Given the size of V_{eff} in the x-y plane (ω_o = 0.34μm), only the central pixels (~50%) in each bacterial cell represent measurements for which it is encompassed in the bacterium (diameter ~0.7 μm). Given the z_o value of 1.4 μm, V_{eff} extends beyond the bacterial cells in the azimuthal direction, and the actual excitation volume, vol_{ex} is that portion of our excitation profile that is contained within the bacterial cell (Figure 2A).

To evaluate the effects of confinement of GFP diffusion in the x,y dimension on measured fluctuations, we performed a 3D Brownian dynamics simulation of a single molecule

diffusing at 10 $\mu m^2/s$ within a bacterial cell of volume 1 fL and within a 0.31 fL diffraction limited 3D Gaussian V_{eff} (Figure 2B). The results of the simulation showed indeed that for our experimental value of ω_o (0.34μm), the effective excitation volume *in cellulo* was 0.07 fL, since by proportionality, with 1 molecule/fL in our simulations, the number of molecules counted by the simulation for a particular value of ω_o corresponds to the excitation volume vol_{ex} (Figure 2D). Moreover, the simulation also showed that the fluctuations (directly related to the molecular brightness ε) were not significantly affected by confinement under our experimental conditions (Figure 2C) (ε=93% of maximum for ω_o=b=0.34 μm, z_0=1.4 μm). Doubling of ω_o leads to a decrease in accuracy to ε=80%. This underscores the importance, of two-photon excitation (which in practice is slightly better than confocal one-photon resolution), as well as the absolute necessity for perfect alignment of the microscope. In eukaryotic cells, a slightly degraded excitation volume will only diminish the fluctuation amplitude and hence the dynamic range of the approach. In bacteria, it precludes making the measurements. The molecular brightness measured in bacteria will be larger than that we would obtain in solution due to the confined geometry in the axial direction (22). However, this increase in ε does not affect our calculations. Confinement in z must be taken into account only if a molecular brightness measured *ex vivo* is compared with a measurement taken *in vivo* or if measurements from different sample thicknesses are to be compared. Since the cell diameter is constant in *B. subtilis* (~0.7 μm) this effect need not be considered for the present study. This is an important advantage for fluctuation techniques in quantifying absolute molecular concentrations in prokaryotes. However, these simulations establish the absolute necessity for diffraction-limited two photon excitation in such studies.

Autofluorescence and detection limits Single molecule detection is commonplace in fluorescence microscopy, hence detection is generally not limited by the number of molecules, but rather by their identity. In single molecule detection of immobile particles, the fluorescence intensity accumulated at a particular location in the image for the immobile molecule of interest exceeds that of the background molecules that are diffusing. Some approaches enhance this difference by incorporating multiple fluorophores at the locus of the molecule of interest. In contrast, in the case of fluctuation microscopy, both the auto-fluorescent species and the molecules of interest diffuse, and hence contribute to the fluctuation signal. The present use of two-photon excitation at 930 nm limits considerably the excitation of the auto-fluorescent molecules compared to visible excitation. We sought to determine the lower detection limit for GFP molecules produced in bacteria using this approach. To do so we measured fluorescent protein production in a *B. subtilis* strain expressing a chromosomal *gfpmut3* gene fused to the promoter of the gluconeogenic *gapB* gene controlled by the CcpN repressor (16) and for which the quantification of basal transcriptional activity under repression had not been accessible to conventional techniques. Depending upon nutrient conditions, the promoter activity of the P_{gapB}*gfpmut3* transcriptional fusion studied here is either strongly repressed (e.g. on glucose) or induced (e.g. on malate)(23).

Two photon microscopy images of the P_{gapB}*gfpmut3* strain grown on glucose consistently showed stronger and more heterogeneous fluorescence signals than did the BSB168 receiver strain (Figure 3A, left panels), indicating that leakage from the gluconeogenic gene promoter did

occur under repressing conditions. Indeed, we were able to carry out FCS measurements on individual cells of the P_{gapB}*gfpmut3 s*train (Figure 3B) in both malate (induced) and glucose (repressed), whereas correlation curves could not be retrieved from data obtained on the receiver strain. Hence, fluctuation techniques in two-photon mode are capable of detecting GFP molecules above the auto-fluorescent background of the cells. However, as can be seen from the inset in Figure 3B and the images in Figure 3C, the degree of photo-bleaching was significant in these single point FCS experiments, particularly under malate where expression was high. Indeed, no fluorescence is detectable after an FCS acquisition inside a bacterial cell due to the fact that the diffusing GFP molecules are confined in the bacterium and therefore more prone to photodamage (Figure 3C, right panel). Hence, reliable determination of molecule numbers by point FCS was not possible. Indeed, to date very few studies have reported the successful use of FCS for quantitative measurements in bacterial cells (24-26). We therefore implemented an alternative method, scanning Number and Brightness (N&B) analysis (11, 12), to measure the absolute concentration of the GFP molecules inside *B. subtilis* cells.

*Cell-by-Cell N&*B In scanning N&B, the moments of the fluctuations at each pixel in a series (50-100) of raster scanned images are used, as in moment analysis (27), to calculate the number and molecular brightness of diffusing fluorescent molecules. In practice the pixel dwell time must be shorter than the diffusion time to avoid averaging, and the detector shot noise must be taken into account (11, 12). Our approach is illustrated in the flow chart in Figure 4 for cells from the strain bearing the un-induced $P_{hyperspank}$ promoter, expressing *gfpmut2*. Using the 50 raster scanned images, the true molecular brightness, ε, can be calculated at each pixel using eq. 4 to provide a pixel based brightness map. Photo-bleaching is much less severe in scanning N&B as compared to single point FCS, since, under our experimental conditions, the laser scans each pixel only once every 4 seconds for a 50 μs dwell time. However, for strains expressing CFP, some photo-bleaching did occur in the N&B measurements, requiring de-trending prior to analysis (11).

In our bacterial samples, the values of the true molecular brightness ε for the FP molecules measured at each pixel present distributions with a mean brightness value between 0.02 and 0.1 photon counts per molecule per 50 μs dwell time (400-2000 counts per second per molecule (cpspm)), depending upon the FP variant used. Given these small values, a considerable proportion of pixel-based ε values in an image are negative. Although they developed true number and brightness analysis (11), in their applications of N&B, Gratton and co-workers typically do not use true N&B maps, but rather the values uncorrected for shot noise (12, 28, 29). Indeed, uncorrected brightness values are sufficient for applications aimed at monitoring changes in molecular brightness linked to changes in stoichiometry of protein complexes. However, in contrast to these previous N&B applications, the present use of N&B seeks to determine absolute values of protein number. For this, correction for shot noise and determination of the true number and brightness are absolutely necessary. Since the brightness of the FP molecules produced from our promoter fusions in bacteria is independent of the concentration and spatial localization, we could perform spatial averaging to improve the precision of the calculations. Using an extension of our PaTrack software (30) all bacterial cells in an image (a single 20 μmx20 μm field of view contains ~ 100-150 single cells) were

automatically detected, and their size and x,y dimensions were recorded. The average molecular brightness, <ε>, for each field of view, was calculated from the pixel-based brightness values (Figure 4). To avoid problems from convolution of the vol_{ex} and to eliminate values outside of cells, we used only those pixels in a particular field of view that were inside of an ellipse of the same center and orientation as the bacterial cells but of ½ the cell area, as this procedure reliably yields > 90% of the true number of molecules. Reduction of central ellipse to ¼ the cell area did not significantly affect the calculation (Figure S1). The brightness values for all cells in the same field of view were averaged and this final average brightness value was used to calculate the pixel based numbers map (Figure 4). Then the cell-based numbers map (Figure 4) was calculated by averaging the n values calculated for the central 50% of the pixels in each cell. Finally, analyses of multiple fields of view under the same conditions were combined to yield a particle numbers histogram (Figure 4) from which the average (<n>) and variance (σ^2_n) for specified promoters and growth conditions can be calculated. For the IPTG inducible *gfpmut2* promoter fusion, in absence of IPTG, and as noted for Figure 1A, the expression levels, and hence numbers histogram is highly heterogeneous and asymmetric, with a small number of cells expressing very high levels of GFP (Figure 4). Bimodal behavior has been observed previously for *lacI* repression in *E. coli* (7), and is apparently similar in the heterologous reporting system in *B. subtilis* used in the present study.

This method for measuring concentration by N&B agreed with FCS measurements for rhodamine 110 solutions in glycerol (Figure S2). One molecule in our *in cellulo* excitation volume vol_{ex} corresponds to a concentration of 24 nM. The average volume of a cell being approximately 1fL (as experimentally determined here), this concentration corresponds to about 17 molecules in the cell. However, since *B. subtilis* cells vary greatly in length, we report the concentration of molecules (expressed as the number of molecules per vol_{ex}) rather than their absolute number. Although the actual protein copy number can be calculated since the cell tracking software provides the information on the size of each cell, we found that this introduces important experimental errors masking biologically relevant cell-cell variations.

<u>*N&B at the detection limits*</u> The pixel-based brightness and numbers maps determined for the BSB168 receiver strain and the P_{gapB}*gfpmut3* fusion strain under strong repression on glucose (Figure 3 A) demonstrate that 2psN&B is capable of counting GFP molecules above the auto-fluorescent background. After analysis (as per the flowchart in Figure 4) of a large number of fields of view for the P_{gapB}*gfpmut3 and* BSB168 strains, we were able to estimate the average cell-based number of GFP molecules produced by the P_{gapB}*gfpmut3* strain under repression. Because the distribution obtained for the FP expressing strain is the sum of the distribution of the background strain and the distribution of FP molecules, the moments for the latter can be obtained by subtraction of the moments of the background strain distribution from those of the FP expressing strain. This yields an average difference of 3 GFP molecules (20.5-17.5) in our vol_{ex} for the repressed P_{gapB}*gfpmut3* strain (corresponding to ~30-50 molecules in the cell). We note that for the background, the average molecular brightness was quite low, 0.022 photons per 50 μs dwell-time per molecule. That found for the repressed P_{gapB}*gfpmut3* strain (0.034 photons per 50 μs dwell-time per molecule) was much lower than that obtained from strains in which the GFPmut3 protein is expressed at reasonably high levels and is concentration independent

(0.1 photons per 50 μs dwell-time per molecule). The low brightness value for the P_{gapB}*gfpmut3* strain on glucose is observed because most cells express very little or no GFP, and for each pixel during each dwell-time there is a high probability to detect zero photons. The data obtained by N&B are insufficient to deconvolve at each pixel, two species with different numbers and brightness values, as can be done with photon counting histograms (31). To check that the low molecular brightness values are not biasing our calculation of GFP molecules, we can estimate the average number of GFP molecules produced by the repressed P_{gapB}*gfpmut3* strain by subtracting the average fluorescence intensity obtained from the BSB168 strain from that obtained for the P_{gapB}-*gfpmut3* strain, and dividing by the known concentration independent molecular brightness, 0.1 counts per 50 μs dwell time per molecule.

$$\langle F\rangle_{PgapB} - \langle F\rangle_{BS168} = \langle F\rangle_{GFP} = \langle n\rangle_{GFP}\varepsilon_{GFP} \quad (6)$$

This calculation yields an average of 3.7 GFP molecules in the vol_{ex}, very close to the value of 3 GFP molecules given above. Thus although for highly repressed promoters we cannot deconvolve the background contribution on a pixel-based or cell-based level, we can obtain the moments of their distributions (the average and the variance in the number of GFP molecules) for a population of cells by subtracting the average and variance of the background numbers distribution from those obtained from distributions of the strains expressing low numbers of GFP molecules.

Experimental Uncertainty and Biological Noise One of the most important results from single cell measurements, in addition to the absolute average expression levels, is the variance or stochastic noise associated with the promoter activity, as noise levels are linked to functional mechanisms of the gene regulation circuits. If we are to evaluate biological noise, it is important to ascertain the extent to which our measurement technique, itself, is uncertain. To do so we analyzed the 2psN&B image stacks obtained for homogeneous solutions of purified mEGFP in 64% glycerol under conditions of laser power, laser dwell time and concentration similar to those for the bacterial cells (Figure S3). In order to compare the same statistics, we calculated the average number and brightness for the homogeneous samples of mEGFP using cell masks from the cell tracking results on the bacteria and the averaging approach for the brightness and the number described above (Figure S3C). While the number of molecules was dependent upon the concentration, as expected, it was independent of the laser power (Figure S3A and B) or laser dwell-time (data not shown). Conversely, also as expected, the brightness depended on laser power but not mEGFP concentration. Most importantly, the percent uncertainty ($\sigma/\langle n\rangle$ was found to be less than 5% (Figure S3D) under our typical conditions of illumination and molecular brightness.

IPTG induction The raster scans corresponding to the average fluorescence images of the *B. subtilis* cells expressing GFPmut2 or CFP from the $P_{hyperspank}$ promoter at different IPTG concentrations as presented in Figure 1 were analyzed by N&B calculating the average cell-based number ($\langle n\rangle$) and brightness ($\langle\varepsilon\rangle$) of molecules as described above (Figure 5A and B). We found that the molecular brightness of CFP was three-fold lower than that of GFPmut2 (0.018 ±

0.003 *vs*. 0.061 ± 0.005 counts per 50 μs dwell time per molecule), explaining at least in part the difference in fluorescence intensities noted above. However, when the fluorescent proteins are highly expressed as in the presence of 100 μM IPTG, the large uncertainty (due to the low fractional fluctuation, <0.08%) in the molecular brightness value precludes accurate calculation of the number of molecules. Thus, we estimate the upper limit for direct 2psN&B under our conditions at ~400 molecules in the observation volume (~10 μM). Above that limit we can use the relationship between average fluorescence intensity and number of molecules obtained at low expression levels to obtain a reliable estimate of the number of molecules at high concentration (Figure 6C, 0.1 and 1 mM IPTG).

The mean number of FP molecules ($\langle n_{FP} \rangle$, Fig. 6C) and the coefficient of variation ($\sigma(n_{FP})/\langle n_{FP} \rangle$) (Figure 6D) observed in the cell population was calculated by subtracting the mean and the variance of the histogram obtained for the background auto-fluorescent molecules from that of the FP producing strains yields. For the un-induced cells carrying the $P_{hyperspank}$*cfp* fusion, our N&B analysis reveals a basal expression level of about 25 CFP molecules per vol_{ex} (~600 nM), although no fluorescence signal was detected above background in bulk assay (Figure 1C). We counted a similar number of the bright GFPmut2 molecules expressed from the same promoter under identical steady-state conditions in the absence of inducer. This reinforces the notion that the difference in average intensity observed for the CFP compared to GFPmut2 in the un-induced strains arises from differences in molecular brightness between the two molecules. After addition of 10 μM IPTG and only 2 hours of growth, the average number of molecules increased about eight fold in the case of GFP, but only five fold in case of CFP. A similar discrepancy is observed in the expression levels of the two fluorescent proteins upon induction at higher IPTG concentration. Under these non-steady state conditions, this discrepancy could reflect a difference in maturation or folding between the two proteins. Given the nearly insignificant differences in nucleotide sequence, it is unlikely that differences in messenger RNA stability play a role.

Interestingly, the population heterogeneity measured by the coefficient of variation ($\sigma(n_{FP})/\langle n_{FP} \rangle$) (Figure 6D) was very large in the un-induced strain (as per the broad and asymmetric histogram in Figure 4), reflecting the highly stochastic nature of expression leakage from the strong $P_{hyperspank}$ promoter under repressing conditions. Upon induction by 10 μM IPTG this heterogeneity decreased drastically, yet remained at a level that is more than 5-fold larger than the experimental error of our measurements (5%). The coefficient of variation at higher inducer concentration (estimated from extrapolation of the numbers vs intensity relationship) decreased even further, ~10% (2-fold the uncertainty of our measurements). This residual noise likely corresponds to "extrinsic noise" arising from-cell-to-cell fluctuations in ribosomes, polymerases, nutrients or other key factors in protein expression and protein and messenger degradation.

Conclusions

Absolute quantification of gene expression is crucial to the modeling of genetic regulatory networks. By using two-photon excitation, by taking into account explicitly the optical and bacterial cell geometries, by selecting appropriate subsets of pixels and by carrying out spatial averaging we have successfully applied fluorescence fluctuation microscopy, and in particular scanning Number and Brightness analysis which nearly eliminates photo-bleaching, to measure absolute concentration of fluorescent proteins and hence promoter activity in *Bacillus subtilis*. We demonstrate the ability of this technique to detect and quantify absolutely very small numbers of fluorescent protein molecules produced from bacterial promoters, above a background of dim auto-fluorescent molecules. Expression from the very strongly repressed P*gapB* promoter tested here had not been previously detected. We have also established the upper limit of this technique to be near 10 μM in fluorescent protein, although reliable estimates above this limit can be obtained using the relationship between average intensity and number of molecules determined at lower concentration. We have determined that the noise levels measured in these living systems are significantly larger than that inherent to the measurement, demonstrating that biological noise can be reliably and quantitatively evaluated by this technique. Two-photon scanning N&B relies on diffusing FPs, which are typically used in investigations of gene regulatory networks. We have shown here and in previous work that GFP, CFP and mCherry (32) can be used simultaneously at the same excitation wavelength, highlighting the feasibility of multi-color experiments. The scanning N&B method does not imply complex data acquisition, beyond the alignment of the microscope to diffraction limited excitation, and the data analysis is straightforward. Given the absolute quantification obtained using this approach, we expect that it will become widely used in future investigations of gene regulatory networks in prokaryotes.

Acknowledgements

The authors would like to thank Enrico Gratton and Michelle Digman for helpful discussions. The work was supported by a grant from the Agence Nationale pour la Recherche (ANR-09-BLAN-0285). M.L.F was supported by postdoctoral fellowships from the National Science Foundation (OISE:IRFP #0710816), European Molecular Biology Organization (ALTF 660-2008) and The European Commission(Marie Curie IIF#237835-InVivoTrnReg).

Reference List

1. Eldar, A., and M. B. Elowitz. 2010. Functional roles for noise in genetic circuits 1. Nature 467: 167-173

2. Kaufmann, B. B., and Van Oudenaarden A. 2007. Stochastic gene expression: from single molecules to the proteome. Curr. Opin. Genet. Dev. 17: 107-112

3. Darzacq, X., J. Yao, D. R. Larson, S. Z. Causse, L. Bosanac, T. de, V, V. M. Ruda, T. Lionnet, D. Zenklusen, B. Guglielmi, R. Tjian, and R. H. Singer. 2009. Imaging transcription in living cells. Annu. Rev. Biophys. 38: 173-196

4. Larson, D. R., R. H. Singer, and D. Zenklusen. 2009. A single molecule view of gene expression. Trends Cell Biol. 19: 630-637

5. Youk, H., A. Raj, and O. A. Van. 2010. Imaging single mRNA molecules in yeast. Methods Enzymol. 470: 429-446

6. Choi, P. J., L. Cai, K. Frieda, and X. S. Xie. 2008. A stochastic single-molecule event triggers phenotype switching of a bacterial cell. Science 322: 442-446

7. Elf, J., G. W. Li, and X. S. Xie. 2007. Probing transcription factor dynamics at the single-molecule level in a living cell. Science 316: 1191-1194

8. Taniguchi, Y., P. J. Choi, G. W. Li, H. Chen, M. Babu, J. Hearn, A. Emili, and X. S. Xie. 2010. Quantifying E. coli Proteome and Transcriptome with Single-Molecule Sensitivity in Single Cells. Science 329: 533-538

9. Elson, E. L. 2004. Quick tour of fluorescence correlation spectroscopy from its inception. J Biomed. Opt. 9: 857-864

10. Haustein, E., and P. Schwille. 2007. Fluorescence correlation spectroscopy: novel variations of an established technique. Annu. Rev. Biophys. Biomol. Struct. 36: 151-169

11. Digman, M. A., R. Dalal, A. F. Horwitz, and E. Gratton. 2008. Mapping the number of molecules and brightness in the laser scanning microscope. Biophys. J. 94: 2320-2332

12. Digman, M. A., P. W. Wiseman, C. Choi, A. R. Horwitz, and E. Gratton. 2009. Stoichiometry of molecular complexes at adhesions in living cells. Proc. Natl. Acad. Sci. U. S. A 106: 2170-2175

13. Rosenfeld, N., T. J. Perkins, U. Alon, M. B. Elowitz, and P. S. Swain. 2006. A fluctuation method to quantify in vivo fluorescence data. Biophys. J 91: 759-766

14. Teng, S. W., Y. Wang, K. C. Tu, T. Long, P. Mehta, N. S. Wingreen, B. L. Bassler, and N. P. Ong. 2010. Measurement of the copy number of the master quorum-sensing regulator of a bacterial cell. Biophys. J 98: 2024-2031

15. Jules, M., L. Le Chat, S. Aymerich, and D. Le Coq. 2009. The Bacillus subtilis ywjI (glpX) gene encodes a class II fructose-1,6-bisphosphatase, functionally equivalent to the class III Fbp enzyme. J. Bacteriol. 191: 3168-3171

16. Botella, E., M. Fogg, M. Jules, S. Piersma, G. Doherty, A. Hansen, E. L. Denham, L. Le Chat, P. Veiga, K. Bailey, P. J. Lewis, J. M. van Dijl, S. Aymerich, A. J. Wilkinson, and K. M. Devine. 2010. pBaSysBioII: an integrative plasmid generating gfp transcriptional fusions for high-throughput analysis of gene expression in Bacillus subtilis. Microbiology

17. Ferguson, M. L., K. Prasad, H. Boukari, D. L. Sackett, S. Krueger, E. M. Lafer, and R. Nossal. 2008. Clathrin triskelia show evidence of molecular flexibility. Biophys. J 95: 1945-1955

18. Benninger, R. K., M. Hao, and D. W. Piston. 2008. Multi-photon excitation imaging of dynamic processes in living cells and tissues. Rev Physiol Biochem. Pharmacol. 160: 71-92

19. Piston, D. W. 1999. Imaging living cells and tissues by two-photon excitation microscopy. Trends Cell Biol. 9: 66-69

20. Cormack, B. P., R. H. Valdivia, and S. Falkow. 1996. FACS-optimized mutants of the green fluorescent protein (GFP). Gene 173: 33-38

21. Williams, R. M., D. W. Piston, and W. W. Webb. 1994. Two-photon molecular excitation provides intrinsic 3-dimensional resolution for laser-based microscopy and microphotochemistry. FASEB J 8: 804-813

22. Macdonald, P., Y. Chen, X. Wang, Y. Chen, and J. D. Mueller. 2010. Brightness analysis by z-scan fluorescence flucuation spectroscopy for the study of protein interactions within living cells. Biophys. J. 99: 979-988

23. Fillinger, S., S. Boschi-Muller, S. Azza, E. Dervyn, G. Branlant, and S. Aymerich. 2000. Two glyceraldehyde-3-phosphate dehydrogenases with opposite physiological roles in a nonphotosynthetic bacterium. J. Biol. Chem. 275: 14031-14037

24. Cluzel, P., M. Surette, and S. Leibler. 2000. An ultrasensitive bacterial motor revealed by monitoring signaling proteins in single cells. Science 287: 1652-1655

25. Le, T. T., S. Harlepp, C. C. Guet, K. Dittmar, T. Emonet, T. Pan, and P. Cluzel. 2005. Real-time RNA profiling within a single bacterium. Proc. Natl. Acad. Sci. U. S. A 102: 9160-9164

26. Meacci, G., J. Ries, E. Fischer-Friedrich, N. Kahya, P. Schwille, and K. Kruse. 2006. Mobility of Min-proteins in Escherichia coli measured by fluorescence correlation spectroscopy. Phys Biol. 3: 255-263

27. Qian, H., and E. L. Elson. 1990. On the analysis of high order moments of fluorescence fluctuations. Biophys. J 57: 375-380

28. Choi, C. K., J. Zareno, M. A. Digman, E. Gratton, and A. R. Horwitz. 2011. Cross-correlated fluctuation analysis reveals phosphorylation-regulated paxillin-FAK complexes in nascent adhesions. Biophys. J 100: 583-592

29. Vetri, V., G. Ossato, V. Militello, M. A. Digman, M. Leone, and E. Gratton. 2011. Fluctuation methods to study protein aggregation in live cells: concanavalin a oligomers formation. Biophys. J 100: 774-783

30. Espenel, C., E. Margeat, P. Dosset, C. Arduise, G. C. Le, C. A. Royer, C. Boucheix, E. Rubinstein, and P. E. Milhiet. 2008. Single-molecule analysis of CD9 dynamics and partitioning reveals multiple modes of interaction in the tetraspanin web. J. Cell Biol. 182: 765-776

31. Chen, Y., J. D. Muller, P. T. So, and E. Gratton. 1999. The photon counting histogram in fluorescence fluctuation spectroscopy. Biophys. J 77: 553-567

32. Savatier, J., S. Jalaguier, M. L. Ferguson, V. Cavailles, and C. A. Royer. 2010. Estrogen receptor interactions and dynamics monitored in live cells by fluorescence cross-correlation spectroscopy. Biochemistry 49: 772-781

Figure Legends

FIGURE 1. Two-photon microscopy imaging of *B. subtilis* cells expressing fluorescent proteins. A) Fluorescence images of cells expressing the *gfpmut2* transcriptional fusion with the $P_{hyperspank}$ promoter after 2 hour induction at the indicated IPTG concentrations. Images are averages of 50 images taken with a laser dwell time of 50 µs. Absolute scales are in photon counts as noted above each image. Fields of view are 20x20 µm. B) Correspondence between average fluorescence measured in individual cells by 2p microscopy imaging (left, pixel-colored bars and axis in average photon counts per pixel) and bulk fluorescence measurements of the bacterial cultures in microplate (right, plain-colored bars and axis in arbitrary units) for cells expressing GFP or CFP under the $P_{hyperspank}$ promoter. C) Fluorescence image of a mixture of *B. subtilis* cells from a GFP producing strain induced at 1 mM IPTG (shown in green) and the BSB168 receiver strain that do not express GFP (shown in grey). Grey color scale is amplified 100x to show the auto-fluorescent background. The fluorescence profiles on the right show cell size (length or diameter) convolved with point spread function (PSF). The profile in the upper panel corresponds to the red dotted line on the image, across two perpendicular GFP-producing cells. In the lower panel, the intensity profile corresponding to the yellow dotted line of the image is shown on two different scales in order to visualize either the two GFP-producing cells (green line) or the two BSB receiver cells (black line).

FIGURE 2. Size and geometry of the point spread function (PSF) relative to the bacterial cytoplasm. A) A schematic showing the size and orientation of the infra-red PSF relative to a 1 fL bacterial cell. The vol_{ex} corresponds to the intersection between the two volumes and taking into account the quadratic dependence of excitation with laser power. B) Simulation of a single molecule diffusing in a three dimensional bacterium of volume 1.0 fL (a=1.5 µm, b=0.35 µm). The molecular trajectory in different colors shows the particle path for the first 0.01 seconds (black), 0.1 seconds (red) and 1 second (green) of the simulation. The particle was given a diffusion coefficient of 10 $\mu m^2/s$ consistent with our FCS measurements of GFP in live bacterial cells. C and D) The dependence of the normalized molecular brightness, ε and the number, n on beam waist, w_0 at the center of the 1 fL cell for a two photon Gaussian excitation volume. The black bar indicates our ω_0 value of 0.34 µm with a normalized brightness of 0.93 in the limit $z_0 >> b$. The number of molecules, n was 0.07 molecules corresponding to a minimum effective excitation volume of 0.07 fL.

FIGURE 3. Detection limits for our 2p fluctuation approach. A) Comparison of two photon imaging and sN&B for the P_{gapB}*gfpmut3* and the BS168 background strains under glucose. Left panel corresponds to average fluorescent intensity images, maximum scale = 1 count/pixel/50 µs laser dwell time; middle panel corresponds to pixel-based molecular brightness maps for BSB168 (top) and P_{gapB}*gfpmut3* (bottom), maximum scale =0.5 counts/molecule; right panel, pixel-based numbers maps for BSB168 and P_{gapB}*gfpmut3* (maximum scale = 80 molecules). B) Fluorescence correlation profiles P_{gapB}*gfpmut3* on glucose (red circles) and malate (blue squares). The inset shows a 5 second fluorescence intensity trace for the two measurements. Baselines due to slow photo-bleaching were subtracted from correlation functions. C)

Fluorescent images of *B. subtilis* P_{gapB}*gfpmut3* strains before (above) and after (below) a typical FCS experiment.

Figure 4: Flow chart for our N&B experiment. The stack of N=50 raster scans of *B. subtilis* cells (Fi) is averaged, <F>. If photo-bleaching is observed, the raster scans are detrended prior to calculations. The fluorescence fluctuations relative to the mean at each pixel are used to calculate the pixel based molecular brightness ε map. Then our Patrack software (30) is used to identify individual bacterial cells and the M central 50% of cellular pixels. The values of ε at these selected pixels are averaged for all cells to yield a single average value of ε for each field of view. This $< \varepsilon >$ is used to calculate the pixel-based numbers map. Then the values of n for the M central 50% of pixels for each cell are averaged to yield a cell-based numbers map. Finally, multiple cells in multiple fields of view are then used to construct the numbers histogram. If the total number of molecules was in the same range as that observed for the reference BSB168 strain, the <n> and σ^2 from the reference strain histogram are subtracted from those of the FP expressing strain histogram to yield the $<n>_{FP}$ and the $\sigma^2(n_{FP})$.

FIGURE 5. Cell-based N&B analysis of the $P_{hyperspank}$ promoter activity in *B. subtilis*. The fluorescence images obtained by 2p fluctuation microscopy for the GFPmut2 or CFP producing strains as shown in Fig. 1, and the BSB168 background strain were analyzed following the flow chart of Fig. 4; <n> is the average number of fluorescent molecules detected in the cells (expressed in number of molecules/vol_{ex}); <e> their average molecular brightness (expressed in counts per molecule per 50 µs dwell time); $<n_{FP}>$ the average number of GFP or CFP deduced after background substraction (expressed in number of molecules/vol_{ex}) and $\sigma(n_{FP})/<n_{FP}>$ is the coefficient of variation of n_{FP} over the mean, reflecting the cell population heterogeneity. Values indicated by an asterix were calculated from fluorescence intensity measurements and brightness values determined at lower concentration. The dotted line indicates the upper limit for N&B analysis.

Figure 1

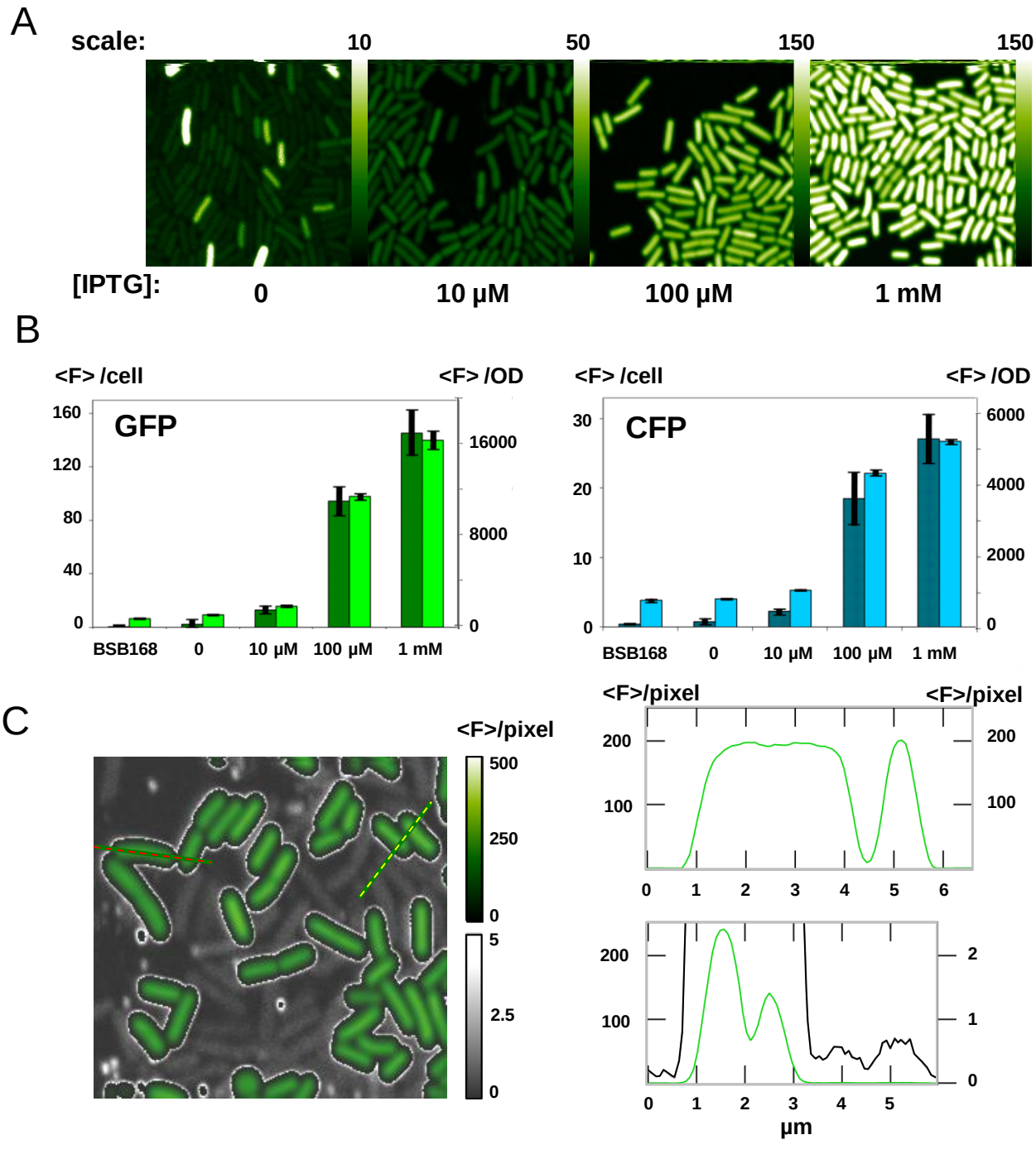

Figure 2

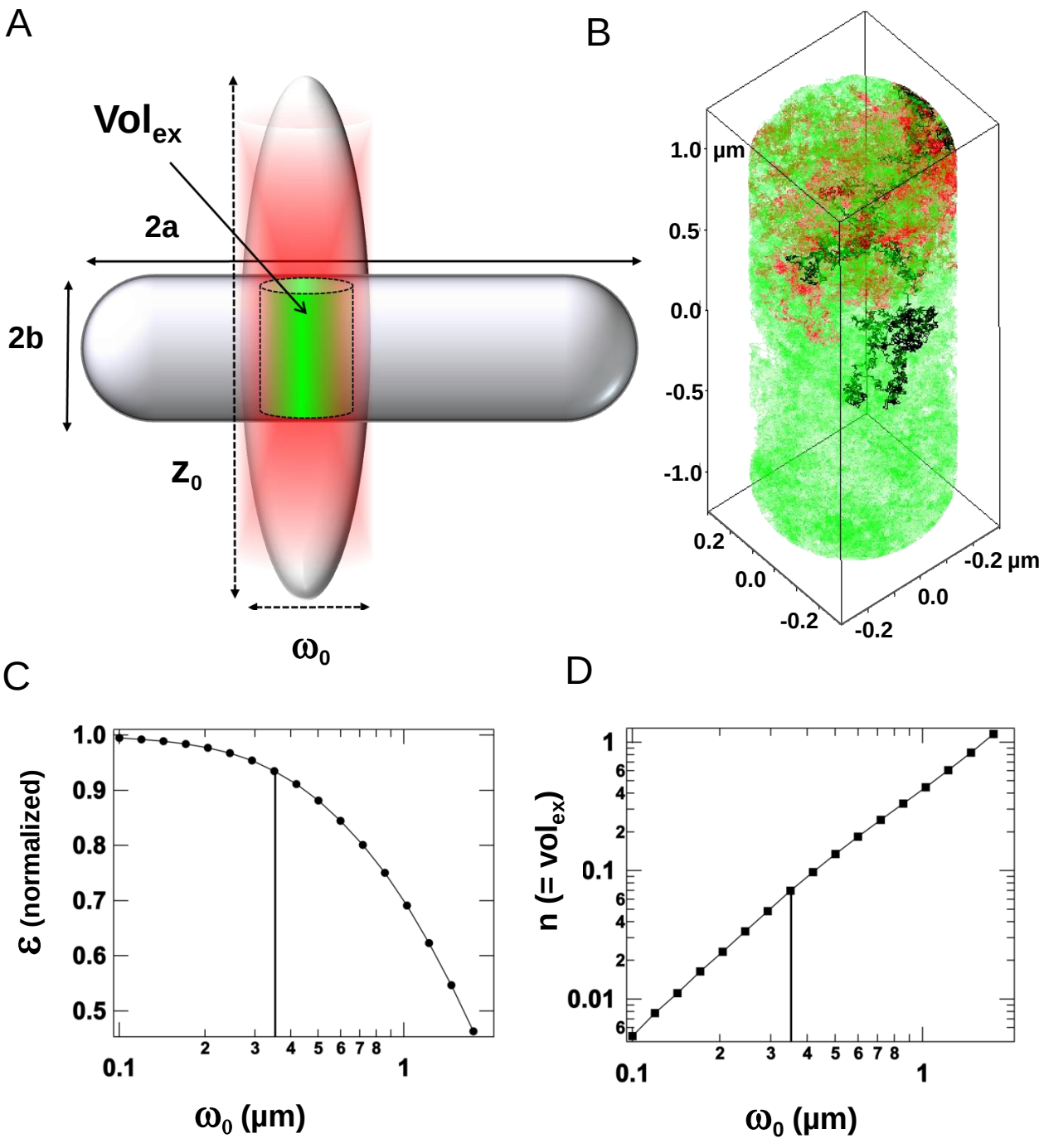

Figure 3

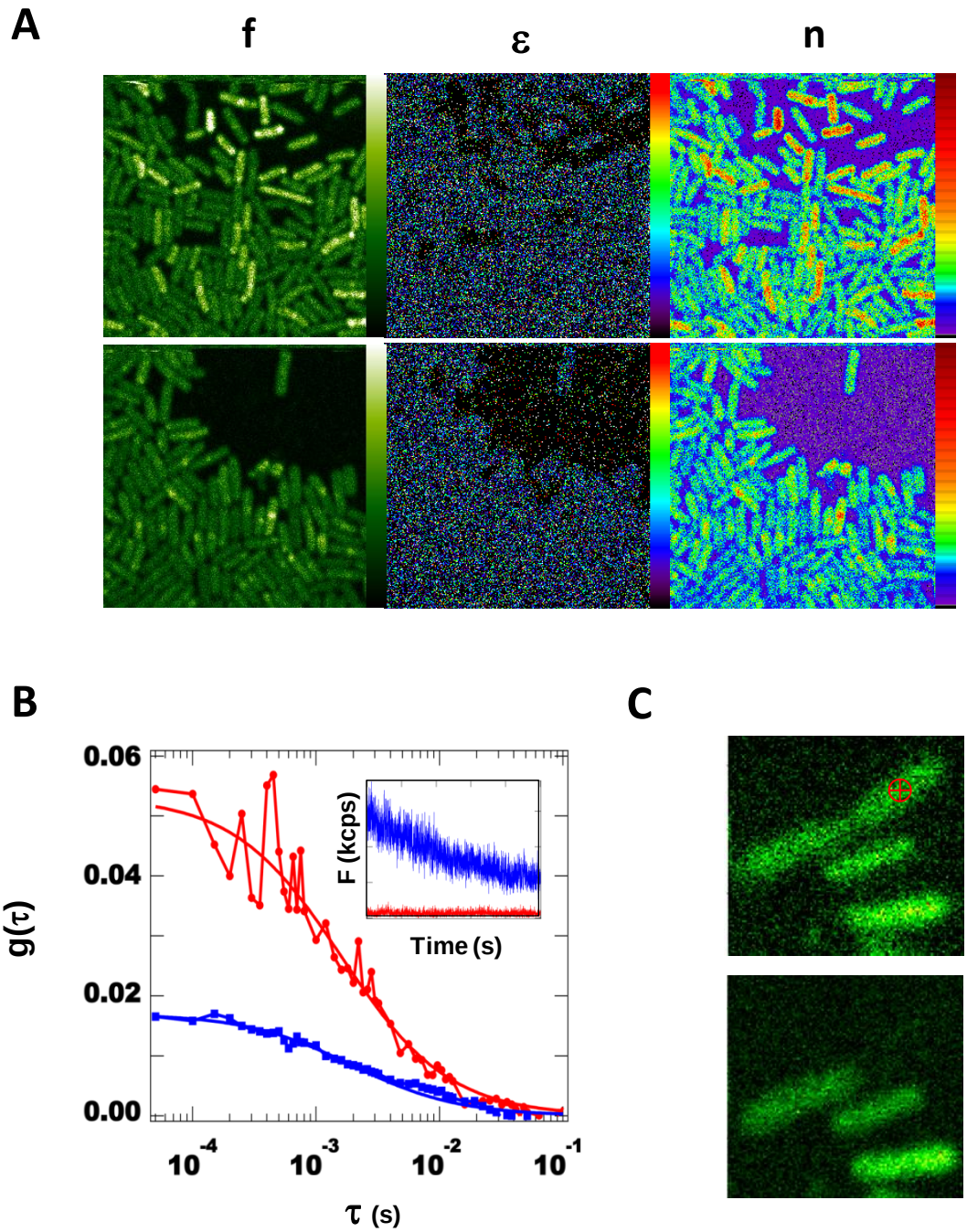

Figure 4

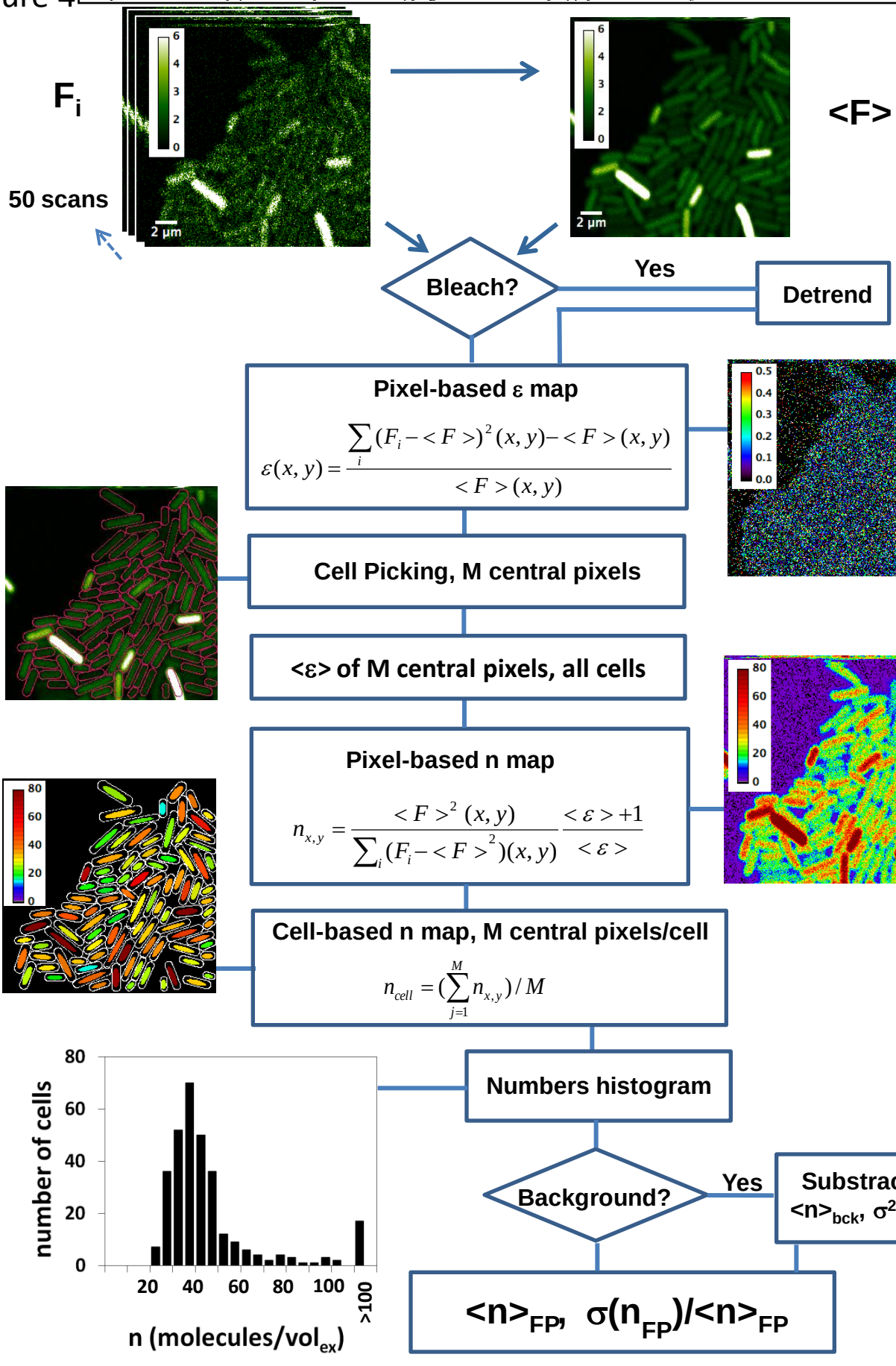

Figure 5